Event-based Adaptive Control of 7-DoF Serial Robot for Teleoperated MIS

Hang Su, Giancarlo Ferrigno, and Elena De Momi
Department of Electronics, Information and Bioengineering, Politecnico di Milano, 20133, Milan, Italy.

***Abstract*—Teleoperated Minimally Invasive Surgery (MIS) can be accomplished with hands-on and teleoperation, where hands-on is required for surgical robot arm docking and instrument insertion, and teleoperation is mandatory for teleoperated surgical operation. Instead of complex instrument operation procedures, we propose a novel continuous adaptive control method to simply the whole workflow for teleoperated MIS. Operation safety and flexibility is validated in a lab setup MIS environment by using the KUKA LWR4+ slave robot and Sigma7 master device. The results show the transition between two modes is smooth and stable.**

***Keywords*—Adaptive control, event based, safe human–robot interaction, teleoperated minimally invasive surgery.**

I. Introduction

The advantages of Minimally Invasive Surgery (MIS) has significantly motivated the development of teleoperated surgical robots in the past decades [1]. In the MIS applications, hands-on control and teleoperation are two basic robot behaviours. "Hands-on": the robot is compliant to be moved by the hand of the user [2]; "Teleoperation": the movement of the robot manipulator is controlled through the master device with a suitable mapping [3]. For all developed surgical robot systems, for example, the neuroArm [4], the Da Vinci robot [5] and the MiroSurge [6], hands-on control is unavoidable for surgical robot arm docking and surgery setup in the operating room [7]. After docking the robot arm and insertion of the surgical tool, the teleoperation is activated for teleoperated surgery. At the end of the teleoperated surgery, surgeon need pull out the instrumentation and move the robot arm back with hands. The traditional workflow involves complex instrument operation. Especially during the teleoperation, if the surgeons find the docking of the surgical arm is not good, switch to hands-on control for redocking and then continue teleoperation is unavoidable. It is easy to annoy diverts the surgeon's attention from the ongoing surgery.

To ease and simply the complex operation procedures, Comparetti et al. proposed to define the device behaviours and switch them from one to another via a Graphical User Interface (GUI) [8]. Nakawala et al. developed a novel context-aware software framework for intelligent surgical training system using knowledge representation, computer vision and semantic web technologies [9]. Tobias et al. modelled and segmented the surgical workflow with laparoscopic video [10]. Kranzfelder et al. performed literature review to identify methods and technologies for increased operating room autonomy[11]. In this paper, we introduce the idea and proposed a novel event-based adaptive control method based on the event. The method automatically transits between hands-on and teleoperation without GUI or complex instrument operation. The effectiveness of the proposed method is validated with a 7-DoF serial robot in a lab setup environment for teleoperated MIS.

This paper is organized as follows: The dynamic model and proposed event-based adaptive control schemes are illustrated in Section II. In Section III, the system description and performance evaluation are presented. And conclusions are drawn in Section VI.

II. Methodology

A. Modelling the serial manipulator

The dynamic model of n-DoF serial manipulator in the Lagrangian formulation can be expressed as:

$$\boldsymbol{M}(\boldsymbol{q})\ddot{\boldsymbol{q}} + \boldsymbol{C}(\boldsymbol{q},\dot{\boldsymbol{q}})\dot{\boldsymbol{q}} + \boldsymbol{g}(\boldsymbol{q}) = \boldsymbol{\tau_c} - \boldsymbol{\tau_{ext}} \quad (1)$$

where $\boldsymbol{q} \in R^n$ is the joint values, $\boldsymbol{M}(\boldsymbol{q}) \in R^{n\times n}$ is the inertia matrix, $\boldsymbol{C}(\boldsymbol{q},\dot{\boldsymbol{q}}) \in R^{n\times n}$ is a matrix representing the Coriolis and Centrifugal effects, and $\boldsymbol{g}(\boldsymbol{q}) \in R^n$ is the gravity torques vector. The torque vectors $\boldsymbol{\tau_c} \in R^n$ and $\boldsymbol{\tau_{ext}} \in R^n$ represent the control torques and the external torque vectors, respectively.

To drive the tool tip, the torque controller is defined as

$$\boldsymbol{\tau_c} = \widehat{\boldsymbol{C}}(\boldsymbol{q},\dot{\boldsymbol{q}})\dot{\boldsymbol{q}} + \widehat{\boldsymbol{g}}(\boldsymbol{q}) + \boldsymbol{\tau_d} \quad (2)$$

where $\widehat{\boldsymbol{C}}(\boldsymbol{q},\dot{\boldsymbol{q}}) \in R^{n\times n}$ and $\widehat{\boldsymbol{g}}(\boldsymbol{q}) \in R^n$ are estimated compensation torques, and $\boldsymbol{\tau_d} \in R^n$ is the control term introduced to conduct the desired surgical tasks.

B. Hands-on and teleoperation

The typical torque control term of the hands-on and teleoperation of the teleoperated MIS are defined and expressed as follows:

1) *Hands-on control:* The human exerts hand force on the robot to move the surgical tip, while the robot becomes passive to be driven by human's intention and movement.

$$\boldsymbol{\tau_d} = -\boldsymbol{D_H}\dot{\boldsymbol{X}} \quad (3)$$

where $\boldsymbol{D_H} \in R^{6\times 6}$ is the diagonal damping matrix and $\dot{\boldsymbol{X}} \in R^6$ is the actual Cartesian velocity. Hand force on the robot could be mapped on the robot arm as extern joints torque $\boldsymbol{\tau_H} \in R^n$, and then the hand force mapped on the end effector can be calculated as $\boldsymbol{F_H}$.

2) *Teleoperation:* The robot is driven to follow a desired trajectory mapped from master device, while the extern force does not intervene the accuracy of the surgical tasks.

$$\boldsymbol{\tau_d} = \boldsymbol{\tau_T} - \boldsymbol{\tau_H} \quad (3)$$

where $\boldsymbol{\tau_H} = \hat{\boldsymbol{\tau}}_{\boldsymbol{ext}} \in R^n$ is the filtered torque from external torque sensors which is mounted into the actuated joints of the Kuka robot, the filtering method is average filter with window length of 5, $\boldsymbol{\tau_T} \in R^n$ is the desired torque to conduct the teleoperated surgical tasks.

For all the MIS task, as it is shown in Fig. 1, the surgical tool held by the robot must go inside the body through a small incision cut made on the patient's body. This kinematic constraint is commonly known as the Remote Centre of Motion (RCM) constraint. The desired Cartesian position from the master device, and the RCM constraint must be simultaneously respected during the surgery. In this paper, an online pose planning scheme is introduced to secure the remote centre motion.

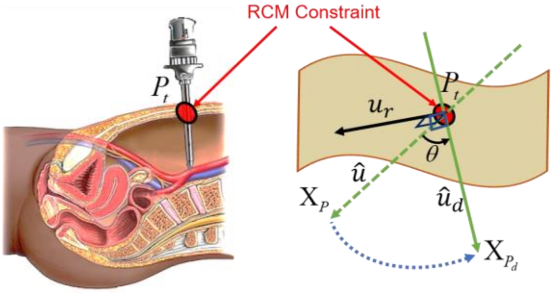

Fig. 1: Minimally invasive surgery: During the MIS, the tool-tip must go through the trocar position $\boldsymbol{P_t}$, representing the RCM Constraint, where $\boldsymbol{X_P}$ and $\boldsymbol{X_{P_d}}$ are the actual and desired Cartesian position inside the abdomen, and θ is the rotation angle between the actual tip direction $\hat{\boldsymbol{u}}$ and the desired tip direction $\hat{\boldsymbol{u}}_d$, $\boldsymbol{u_r}$ is the rotation axis of $\hat{\boldsymbol{u}}$ and $\hat{\boldsymbol{u}}_d$.

The operational coordinates $\boldsymbol{X} = [\boldsymbol{X_P}, \boldsymbol{X_R}]^T \in R^6$ are the actual tip pose, including the actual tool-tip position $\boldsymbol{X_P} = [x, y, z]$ and the actual tool orientation expressed by with Euler angle $\boldsymbol{X_R} = [\alpha, \beta, \gamma]$. $\mathbf{X_d} = [X_{P_d}, X_{R_d}]^T \in R^6$ is the desired tip pose, where $\boldsymbol{X_{P_d}} = [x_d, y_d, z_d]$ is the desired Cartesian position given by the master device and the desired orientation $\boldsymbol{X_{R_d}} = [\alpha_d, \beta_d, \gamma_d]$ is calculated based on X_P online in order to guarantee the tip going through the trocar position $\boldsymbol{P_t} = [x_t, y_t, z_t]$ during the movement, as follows:

The rotation angle θ (see Fig. 1) between the actual tool direction $\hat{\boldsymbol{u}}$ and the desired tool direction $\hat{\boldsymbol{u}}_d$ can be calculated as $\theta = \arctan\frac{\hat{\boldsymbol{u}}_d \times \hat{\boldsymbol{u}}}{\hat{\boldsymbol{u}}_d \cdot \hat{\boldsymbol{u}}}$. The unit vector describing the rotation axis $\boldsymbol{u_r} = [u_x, u_y, u_z]$ from $\hat{\boldsymbol{u}}$ to $\hat{\boldsymbol{u}}_d$ is defined by $\boldsymbol{u_r} = \frac{\hat{\boldsymbol{u}}_d \times \hat{\boldsymbol{u}}}{\|\hat{\boldsymbol{u}}_d \times \hat{\boldsymbol{u}}\|}$. A Skew-symmetric matrix is introduced as:

$$\boldsymbol{\Gamma} = \begin{bmatrix} 0 & -u_z & u_y \\ u_z & 0 & -u_x \\ -u_y & u_x & 0 \end{bmatrix}$$

Finally, the desired orientation matrix $\boldsymbol{R_d}$ can be calculated using

$$\boldsymbol{R_d} = \boldsymbol{I} + \boldsymbol{\Gamma} sin(\theta) + 2\boldsymbol{\Gamma}^2 sin^2\left(\frac{\theta}{2}\right) \cdot \boldsymbol{R} \tag{4}$$

where $\boldsymbol{R}$ is the actual rotation matrix. It is easy to get $\boldsymbol{X_{R_d}}$ with Euler transformation from rotation matrix $\boldsymbol{R_d}$.

To reach the desired tip pose $\boldsymbol{X_d}$, task-space dynamic with Cartesian impedance control $\boldsymbol{\tau_T} \in R^n$ is introduced as

$$\boldsymbol{\tau_T} = \boldsymbol{J^T}\left(\left(\frac{\partial V(q)}{\partial X}\right)^{\boldsymbol{T}} - \boldsymbol{D_X}\dot{\boldsymbol{X}}\right) \tag{5}$$

based on the potential function of a virtual spring and a damping term, as used in [12], where $\boldsymbol{J} \in R^{6\times n}$ is the Jacobian matrix, $\boldsymbol{D_X} \in R^{6\times 6}$ is the diagonal damping matrix and the virtual potential function $V(\boldsymbol{q}) \in R$ is defined based on the difference between the desired and the actual Cartesian trajectory $\widetilde{\boldsymbol{X}}(\boldsymbol{q}) = \mathbf{X_d} - \boldsymbol{X}(\boldsymbol{q})$, as follows:

$$V(\boldsymbol{q}) = \frac{1}{2}\widetilde{\boldsymbol{X}}^{\boldsymbol{T}}(\boldsymbol{q})\boldsymbol{K_X}\widetilde{\boldsymbol{X}}(\boldsymbol{q}) \tag{6}$$

where $\boldsymbol{X}(\boldsymbol{q})$ is the actual target pose calculated from the forward kinematic function, $\boldsymbol{K_X} \in R^{6\times 6}$ is the is the diagonal stiffness matrix. For simplification, we assume that the surgical robot is far away from its singularity and the pseudoinverse of $\boldsymbol{J}$ exists.

C. *Event-based adaptive control scheme*

According to the general MIS scenario and workflow [10], the surgical robot behaviour should be based on the actual human event in the surgery. To serve as an intelligent surgical arm, the robot should be intuitive to the surgical event. Compared with camera or other sensor, position and force are two reliable information sources for robot arm in the complex environment of the operating room. Hence, we propose to define the control modes according to the position $\boldsymbol{X}$ of the tool tip and hand force $\boldsymbol{F_H}$ on the end effector of the robot.

1) *Adaption based on tool tip position $\boldsymbol{X}$:*

As it is shown in Fig. 2, the robot control modes can be classified based on three main areas: (A) when the surgical tool is out of the patients' abdomen, hands-on control should be utilized for robot arm docking. (B) In the abdomen, there should be a transition area, where the tool tip should be not only control by hand, also for teleoperation. Hands-on is for tool tip insertion. Teleoperation is for reaching the target. (C) In the abdomen, teleoperation should work near the organ target, and hands-on should be constrained to avoid hurt important organ. The transition between A and C should be smooth and safe.

To distinguish which area the tool tip is in, we define the

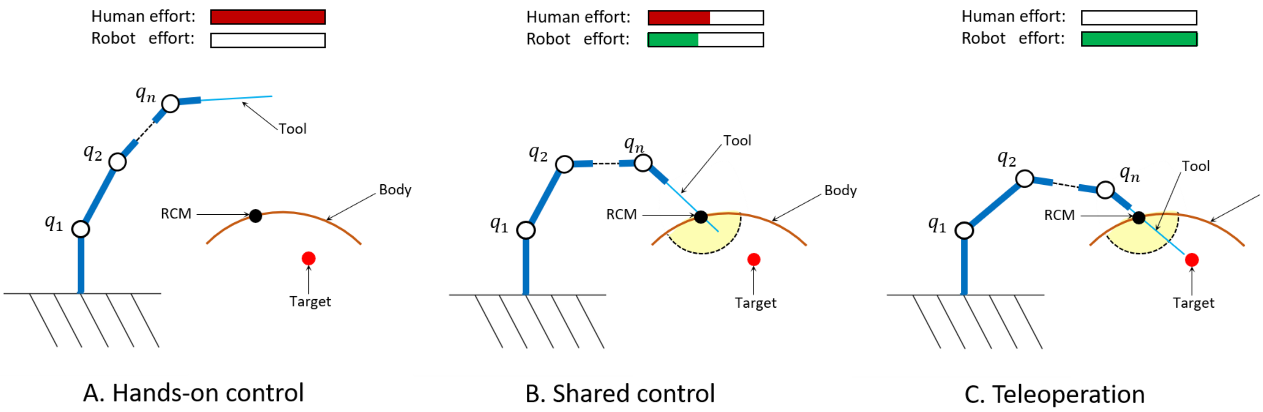

Fig. 2: Human interaction during teleoperated minimally invasive surgery

yellow transition area is a part of sphere, its origin is the RCM constraint $\boldsymbol{P_t}$, and its radius is l. Then a parameter d is introduced as

$$d = (\boldsymbol{X}(\boldsymbol{q}) - \boldsymbol{P_t}) \cdot \hat{\boldsymbol{u}} \quad (7)$$

where $\boldsymbol{X}(\boldsymbol{q})$ is the actual Cartesian position and $\hat{u}$ is the actual tip direction. To achieve smooth and safe transition, an adaptive weight function is defined as:

$$W_1(d) = \left(\frac{1-\cos(\min[\max[0,d],l]*\pi/l)}{2}\right)^{\sigma_1} \quad (8)$$

where $\sigma_1 \in R^+$ is a positive index for adaptive weight distribution, l is the radius of the transition area; $W_1(d) \in R$ is the weight function, and $0 \leq W_1(d) \leq 1$ .The corresponding illustration of the weight distribution can be seen in Fig. 3. The adaptive controller based on position can be expressed as

$$\boldsymbol{\tau_d} = W_1(d)(\boldsymbol{\tau_T} - \boldsymbol{\tau_H}) - (1 - W_1(d))\boldsymbol{D_H}\dot{\boldsymbol{X}} \quad (9)$$

2) Adaption based on hand force $\boldsymbol{F_H}$:

Safety and accuracy are always the most critical concerns during the teleoperated surgery. In the normal case during the teleoperation, the tool tip should be controlled only by master device without influence from extern force. However, if there is something unexcepted happened, for example, error teleoperation, master device fault, it is essential to pull the surgical tip out from the abdomen as soon as possible. The robot could know this based on the extern force sensor.

We proposed to adopt the magnitude of the force $\|\boldsymbol{F_H}\|$ as the parameter to adaptive change the robot behaviour. The corresponding adaptive weight function is defined as:

$$W_2(\|\boldsymbol{F_H}\|) = 1 - \frac{1}{1+e^{-\sigma_2(\|\boldsymbol{F_H}\|-M)}} \quad (10)$$

where $\sigma_2 \geq 3 \in R^+$ is a positive index for adaptive weight distribution, M is the threshold value for transition; $W_2 \in R$ is the weight function, and $0 \leq W_2 \leq 1$ The corresponding illustration of the weight distribution can be seen in Fig. 3. The adaptive controller based on hand force can be expressed as

$$\boldsymbol{\tau_d} = W_2(\|\boldsymbol{F_H}\|)(\boldsymbol{\tau_T} - \boldsymbol{\tau_H}) - (1 - W_2(\|\boldsymbol{F_H}\|))\boldsymbol{D_H}\dot{\boldsymbol{X}} \quad (11)$$

In conclusion, the final proposed control scheme based on the tool tip position and the hand force can be expressed by

$$\boldsymbol{\tau_d} = W_1 W_2(\boldsymbol{\tau_T} - \boldsymbol{\tau_H}) - (1 - W_1 W_2(\|\boldsymbol{F_H}\|))\boldsymbol{D_H}\dot{\boldsymbol{X}} \quad (12)$$

And the whole control block diagram is show in Fig. 4.

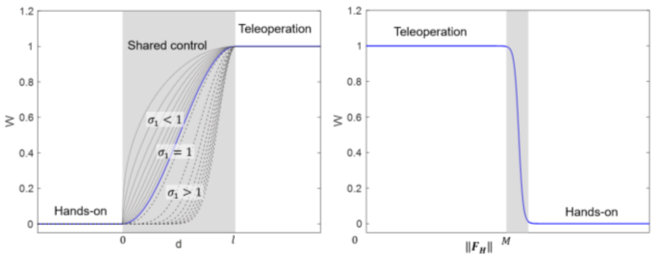

Fig. 3: Illustration of weight function $W_1(d)$ and $W_2(\|\boldsymbol{F_H}\|)$, (a) $W_1(d)$ transits smoothly between 0 and 1, and $W_1(d) = 0$ and $W_1(d) = 1$ correspond to the modes of hands-on control and teleoperation, respectively; $W_2(\|\boldsymbol{F_H}\|)$ also transits smoothly between 0 and 1, and $W_2(\|\boldsymbol{F_H}\|) = 0$ and $W_2(\|\boldsymbol{F_H}\|) = 1$ correspond to the modes of hands-on control and teleoperation, respectively; (b) σ_1 and σ_2 determines the distribution shape of the weight distribution of the weight function.

III. Performance Evaluation

A. System Description

The developed teleoperated MIS system is shown in Fig. 5. A redundant robot (LWR4+, KUKA, Germany) serves as the slave manipulator torque-controlled through Fast Research Interface (FRI), which provides direct low-level real-time access to the robot controller (KRC) at rates of 500 Hz [13]. The teleoperation scheme implements position control for 3D Cartesian coordinates with a master device (Sigma 7, Force Dimension, Switzerland) in our previous work [14]. The orientation degrees of freedom of the end-effector are determined by the RCM constraint, explained in Section II.

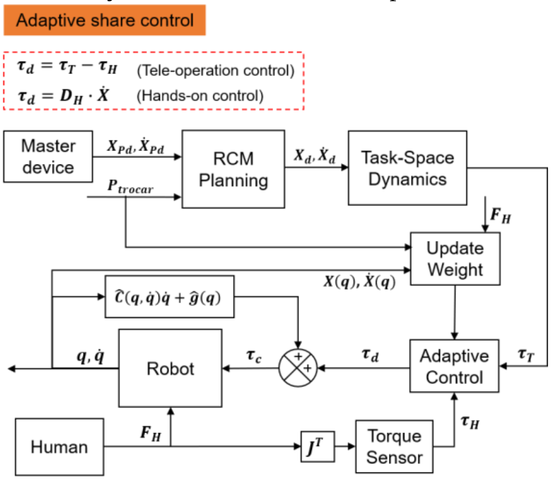

Fig. 4: Control diagram of the proposed adaptive control scheme.

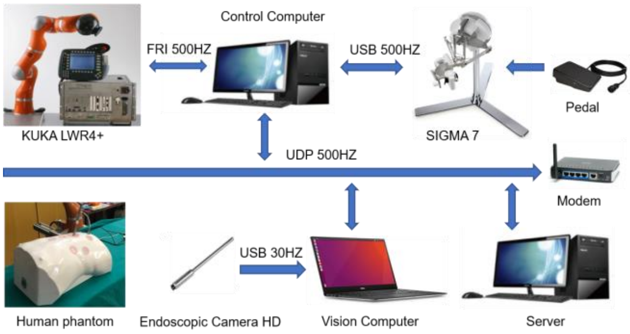

Fig. 5: Overview of the tele-operated surgical robot control system

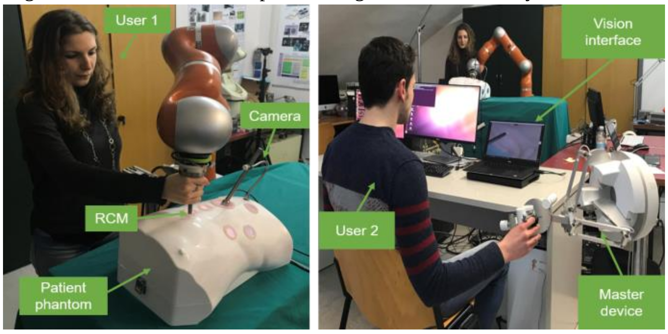

Fig. 6: Experimental set up scene

For system validation, a lab setup human phantom is adopted to simulate the MIS task. An endoscopic camera HD (720p, 30Hz) is used to for vision. A human patient phantom with the similar size of real human for MIS is adopted.

B. Experimental protocol

Two healthy users were enrolled to setup the experimental scene with the developed teleoperated MIS system. As it is shown in Fig. 6, user 1 is command to control tool tip with hand and then user 2 works on the teleoperated MIS tasks. To test the feasibility of the developed method, the normal MIS surgical workflow is conducted for 10 times. For each test, it includes five procedures. (I: hands-on move the tool-tip outside of the abdomen; II: hands-on to pull out the tip from the shared control area; III; teleoperation in the shared control area and teleoperation area after hands-on; IV: a suitable hand force in teleoperated area; V: a big force in teleoperated area to pull the tool-tip out from the abdomen).

In the experiment, $l = 0.08\text{m}$, $\sigma_1 = 3$, $\boldsymbol{D_H} = diag\ [5,5,5,0.3,0.3,0.3]\ Ns/m$, $M = 2.35N$, $\sigma_2 = 5$, $\boldsymbol{D_X} = diag[3000,3000,\ 3000, 300, 300,\ 300]\ \ Ns/m$, $\boldsymbol{K_X} = diag\ [30,30, 30,3.5,3.5,\ 3.5]\ N/m$. During the whole procedure, hands on force $||\boldsymbol{F_H}||$, teleoperation force $||F_T||$ is force mapped from $\boldsymbol{\tau_T}$ on the end effector and the tool tip trajectory $\boldsymbol{X} = (x, y, z)$ are collected. The parameter d and adaptive weight W are also recorded.

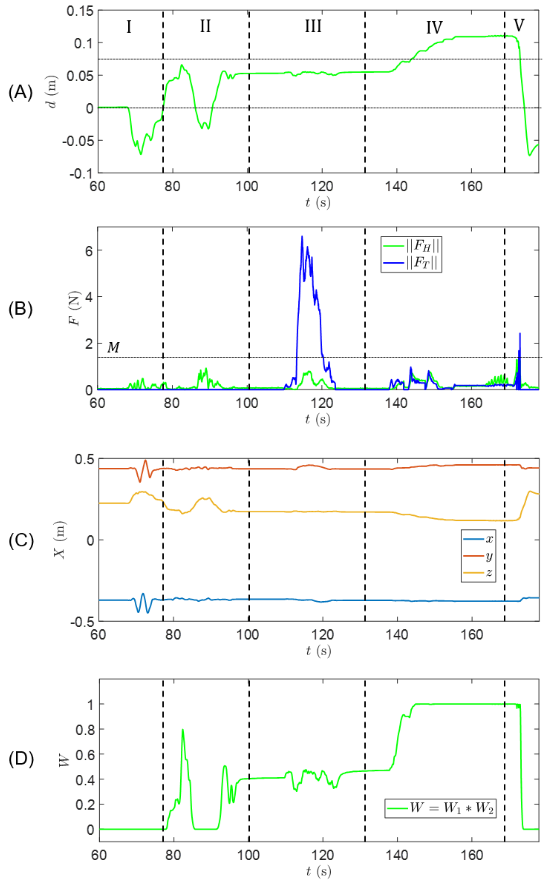

Fig. 7: Experiment results: (A) Variation of the insertion parameter d; (B) hands-on force and teleoperation force; (C) tool tip trajectory; (D) adaptive weight W.

C. Experiment results

The whole surgical procedures are conducted, and corresponding experimental results are shown in Fig. 7. It includes 5 procedures： I. hands-on can move the tool-tip into and outside of the abdomen; II. hands-on can pull out the tip from the shared control area; III. teleoperation works in the shared control area and teleoperation area; IV. a suitable hand force in teleoperated area without change the position of the tool tip; V. a big force on the tool tip in teleoperated area can pull the tool-tip out from the abdomen.

The robot behaviour is automatically switched based on the tool tip position. d divides the working area into three different areas for hands-on control, shared control and teleoperation. M secures the biggest extern force during the teleoperation. The whole surgical workflow can be done with a suitable setting of d and M based on the surgeons' real experience.

IV. Conclusion

The presented scheme provides a novel solution to address the switching of working procedures in teleoperated MIS. Instead of designing multiple controllers and switching between them with instrument operation or GUI command. It developed a unified formulation which integrates hands-on control and teleoperation for teleoperated MIS. It eases the surgeons' work and enhance the safety for the surgery.

However, in this work, we adopt torque sensor to measure and map the hand force on the surgical tip, which is not adequate for complete clinical surgical application. We would install a 6D force sensor on the tool tip to achieve the hands-on force measurement in the following work.

References

[1] A. R. Lanfranco, A. E. Castellanos, J. P. Desai, and W. C. Meyers, "Robotic surgery: a current perspective," *Annals of surgery,* vol. 239, no. 1, p. 14, 2004.

[2] E. Beretta, E. De Momi, F. Rodriguez y Baena, and G. Ferrigno, "Adaptive hands-on control for reaching and targeting tasks in surgery," *International Journal of Advanced Robotic Systems,* vol. 12, no. 5, p. 50, 2015.

[3] N. ENAYATI, "Adaptive shared-control in surgical robotics," *Polimi,* 2017.

[4] G. R. Sutherland, I. Latour, and A. D. Greer, "Integrating an image-guided robot with intraoperative MRI," *IEEE engineering in medicine and biology magazine,* vol. 27, no. 3, pp. 59-65, 2008.

[5] G. S. Guthart and J. K. Salisbury, "The Intuitive/sup TM/telesurgery system: overview and application," in *Robotics and Automation, 2000. Proceedings. ICRA'00. IEEE International Conference on*, 2000, vol. 1, pp. 618-621: IEEE.

[6] U. Hagn *et al.*, "DLR MiroSurge: a versatile system for research in endoscopic telesurgery," *International journal of computer assisted radiology and surgery,* vol. 5, no. 2, pp. 183-193, 2010.

[7] P. Iranmanesh, P. Morel, O. J. Wagner, I. Inan, F. Pugin, and M. E. Hagen, "Set‐up and docking of the da Vinci® surgical system: prospective analysis of initial experience," *The international journal of medical robotics and computer assisted surgery,* vol. 6, no. 1, pp. 57-60, 2010.

[8] M. D. Comparetti, E. Beretta, M. Kunze, E. De Momi, J. Raczkowsky, and G. Ferrigno, "Event-based device-behavior switching in surgical human-robot interaction," in *Robotics and Automation (ICRA), 2014 IEEE International Conference on*, 2014, pp. 1877-1882: IEEE.

[9] H. Nakawala, G. Ferrigno, and E. De Momi, "Development of an intelligent surgical training system for Thoracentesis," *Artificial intelligence in medicine,* 2017.

[10] T. Blum, H. Feußner, and N. Navab, "Modeling and segmentation of surgical workflow from laparoscopic video," in *International Conference on Medical Image Computing and Computer-Assisted Intervention*, 2010, pp. 400-407: Springer.

[11] M. Kranzfelder *et al.*, "Toward increased autonomy in the surgical OR: needs, requests, and expectations," *Surgical endoscopy,* vol. 27, no. 5, pp. 1681-1688, 2013.

[12] A. Dietrich, T. Wimbock, A. Albu-Schaffer, and G. Hirzinger, "Integration of reactive, torque-based self-collision avoidance into a task hierarchy," *IEEE Transactions on Robotics,* vol. 28, no. 6, pp. 1278-1293, 2012.

[13] G. Schreiber, A. Stemmer, and R. Bischoff, "The fast research interface for the kuka lightweight robot," in *IEEE Workshop on Innovative Robot Control Architectures for Demanding (Research) Applications How to Modify and Enhance Commercial Controllers (ICRA 2010),* 2010, pp. 15-21: Citeseer.

[14] N. Enayati, G. Ferrigno, and E. De Momi, "Skill-based human–robot cooperation in tele-operated path tracking," *Autonomous Robots,* pp. 1-13, 2017.